Hindawi
Advances in Materials Science and Engineering
Volume 2018, Article ID 2524748, 9 pages
https://doi.org/10.1155/2018/2524748

Research Article

Simulation and Experimental Study on Properties of Ag/SnO_2 Contact Materials Doped with Different Ratios of Ce

Jingqin Wang, Ying Zhang, and Huiling Kang

State Key Laboratory of Reliability and Intelligence of Electrical Equipment, Hebei University of Technology, Tianjin 300130, China

Correspondence should be addressed to Ying Zhang; 13512474229@163.com

Received 1 August 2018; Revised 3 September 2018; Accepted 4 September 2018; Published 8 October 2018

Academic Editor: Alfredo Juan

SnO_2 in the Ag/SnO_2 contact material is a kind of high hardness and almost insulated wide bandgap semiconductor material. In the process of use, the contact resistance is larger and the temperature rise is higher, which reduces the reliability of contacts and shortens the electrical life. In order to improve the properties of Ag/SnO_2 contact materials, based on the first principle of density functional theory, this paper presents a method of doping SnO_2 with the calculation of different proportions of rare earth Ce electrical and mechanical properties. The results of energy band, density of state, and elastic constant show that when the doping ratio of Ce is 0.125, the electron mobility is the highest, the conductivity is the best; the hardness decreases, and the universal elastic anisotropy index is the smallest. Finally, in the experiment, SnO_2 powders with different doping ratios are prepared by the sol-gel method, and Ag/SnO_2 contacts with different doping proportions are prepared by powder metallurgy. Arc energy, contact resistance, and hardness are measured; scanning electron microscopy was used to observe and analyze the surface morphology. The final simulation and experimental results are well matched.

1. Introduction

The contact resistance and the temperature rise in the process of using automotive relay contacts are increased, making life expectancy to decrease [1–3]. This is because SnO_2 in Ag/SnO_2 contact material is a kind of wide bandgap semiconductor material, which is almost insulator [4]. At the same time, SnO_2 is a high hardness brittle reinforcing phase, making contact material processing and composite molding extremely difficult. The study shows that the doping modification of Ag/SnO_2 with rare earth materials is a good method to solve the above problems [5].

For now, improving the performance of Ag/SnO_2 contact materials by doping is still in the experimental stage. How to get the best performance by doping with the proper amount of rare earth elements depends on the original experiments and experience, and there are some difficulties in the preparation of samples and the accuracy of experimental equipment, which restrict the development of Ag/SnO_2 materials.

Zhu Yancai and others in the study on new type of $Ag/SnO_2/CeO_2$ electrical contact material preparation and electrical properties found that CeO_2-doped Ag/SnO_2 improved electrical performance [6]. From the experimental point of view, they had only selected a single ratio of doping, not knowing the best proportion of doping to get better performance. In the study of the structure and optical properties of Ce-doped SnO_2, Shan Linting et al found that the Ce-doped SnO_2 makes conduction band bottom to move toward the low-energy side, the bandgap becomes smaller, and the conductivity increases [7]. The conductivity was only studied by simulation calculations.

Wang Qingwei et al found that CeO_2-doped SnO_2 when doping too little is not conducive to the sintering and growth of tin oxide crystals, while excessive doping will prevent the lattice growth and affects the stability of the lattice, easily leading to serious cracking of the product [8, 9]. So, the doping amount of CeO_2 should be controlled.

It is of great significance to understand the basic properties of Ag/SnO_2 contact material. In this paper, based

on the first-principles calculation of density functional theory [10], different proportions of rare earth Ce are doped into the contact material of SnO_2, conducting geometric optimization, energy band, density of states and elastic constant, and then analyzing the conductivity and hardness to theoretical study the electronic structure and mechanical properties.

2. Cell Model and Calculation Method

2.1. Cell Model. In this paper, we had constructed a SnO_2 primary cell model, as shown in Figure 1(a). SnO_2 (cassiterite) has the rutile structure space group P42/mnm [11]. Each SnO_2 contains 2 Sn atoms and 4 O atoms. The atomic substitution method was used to construct the supercell model $Sn_{1-x}Ce_xO_2$ ($x = 0$, 0.083, 0.125, and 0.167). Table 1 shows the relationship between the doping ratio and the supercell. Taking the doping ratio of 0.125 as an example, the $1 \times 2 \times 2$ supercell model of SnO_2 is established and one of the Sn atoms is replaced by a rare earth atom Ce, as shown in Figure 1(b).

2.2. Calculation Method. In this article, we used Materials Studio software and completed the calculation by using the CASTEP module. The calculation process uses periodic boundary conditions based on DFT [12]. Since generalized gradient approximation (GGA) considers the effect of charge density near a certain location on the exchange-correlation energy, for example, taking into account the effect of the first-order gradient of density to correct local variations, it is possible to properly correct the effects of charge density regions exponential form; in the geometric optimization, energy band and density of state calculations have achieved good results [13].

The local density approximation (LDA) assumes that the nucleus spacing in the system is far apart, and the motion of electrons in its lattice background can be approximated as a behavior in a uniform field. It is suitable for the calculation of the ground state properties of various systems, and very good results are achieved when calculating the elastic properties of the system [14]. Therefore, the geometric optimization process uses the PBE method under GGA; the CA-PZ method under LDA is used to calculate the elastic constants in the mechanical properties on the basis of optimization. For geometric optimization, energy band, density of states, and elastic constants are calculated adopting the plane wave ultrasoft pseudopotential (Ultrasoft) method.

In order to compare the calculated results of SnO_2 doped with different proportions of Ce, the parameters of software simulation are set to be consistent. The calculated parameters are as follows: the cutoff energy of the plane wave is 370 eV, the SCF tolerance is 1.0×10^{-6} eV/atom, and the K point in the Brillouin region is $5 \times 5 \times 8$. The calculation process is carried out in the reciprocal space.

3. Results and Discussion

3.1. Crystal Structure. The crystal parameters of geometry optimization and experimentation of SnO_2 doped with different proportions of Ce are optimized, and the parameters after optimization are shown in Table 2.

According to the optimization results, the experimental values and calculated values of the lattice parameters of Ce-doped SnO_2 with different proportions are not much different. The lattice constant and volume of SnO_2 after doping have different growth degrees compared with SnO_2, which is consistent with Vegard's law [15], indicating that the calculation results are reliable. This shows that doping Ce can cause slight distortion of the crystal structure and thus can adjust the structural parameters of SnO_2, thereby improving the performance of SnO_2.

3.2. Conductivity

3.2.1. Density of States and Electron Concentration. The density of states of SnO_2 and SnO_2 doped with different proportions of rare earth Ce is shown in Figure 2. Figure 2(a) shows the density of states of SnO_2, and Figures 2(b)–2(d) show the density of states of SnO_2 with the Ce doping ratios of 16.7%, 12.5%, and 8.34%, respectively. The Fermi level is chosen to be zero of the energy scale. The energy level above the Fermi surface (0 eV) is the conduction band, and the energy level below the Fermi surface is the valence band.

It can be seen from Figure 2 that the density of states undoped and doped with different ratios of Ce shows that the Fermi surface of the SnO_2 supercell after doping moves to the valence band in different degrees, while the conduction band of undoped SnO_2 is about 0 eV–20 eV, and the conduction band of SnO_2 is about 0 eV–7 eV after doping. The conduction band is narrowed, which indicates that the SnO_2 model after different ratios of doping enhances the electronic state near the Fermi level, and more partial waves cross the Fermi level, the interaction between electrons is enhanced, and the conductivity is enhanced.

The Fermi surface of the Ce-doped SnO2 supercell with different ratios of rare earth elements enters the conduction band to a different extent, which indicates that the relative electron concentration entering the conduction band of SnO2 supercell is different. The relative number of electrons entering the conduction band can be obtained by integrating the density of states of Figures 2(a)–2(d) by Origin software. The obtained $Sn_{1-x}Ce_xO_2$ ($x = 0.083$, 0.125, 0.167) is shown in Table 3.

As can be seen from Table 3, the higher the doping concentration, the higher the relative electron number into the conduction band and the higher the concentration of relative electron.

The conductive performance of the material can be expressed by the conductivity δ_i. The conductivity of the material by semiconductor physics theory is [16]

$$\delta_i = n_i q \mu_i, \tag{1}$$

where q is the electron charge constant, and the conductivity is proportional to the electron concentration n_i and the electron mobility μ_i, which can be obtained from the above formula.

In addition to being affected by the relative number of electrons, the conductivity is also affected by the electron

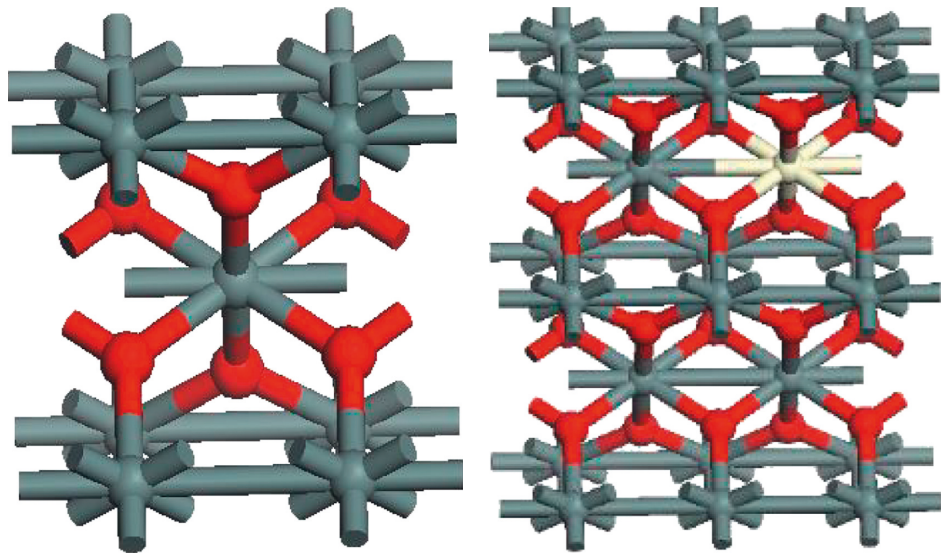

(a) (b)

Figure 1: Cell model (a) SnO_2 and (b) Ce-doped SnO_2.

Table 1: Doping ratio and supercell correspondence.

Supercell	Doping ratio
$1 \times 1 \times 3$	16.7%
$1 \times 2 \times 2$	12.5%
$1 \times 2 \times 3$	8.34%

Table 2: Doping ratio and crystal structures.

	Model	$1 \times 1 \times 3$ 16.7%	$1 \times 2 \times 2$ 12.5%	$1 \times 2 \times 3$ 8.3%
a	Experiment value	4.737	4.737	4.737
	Calculated value	4.958	4.951	5.007
b	Experiment value	4.737	4.737	4.737
	Calculated value	4.958	4.948	4.986
c	Experiment value	3.186	3.186	3.186
	Calculated value	3.346	3.327	3.317
Volume	Experiment value	214.202	285.965	428.947
	Calculated value	246.751	326.013	496.851

mobility. According to the characteristics of the CASTEP software. When applying the first-principles study, the software sets the temperature to a low temperature of 0 K. According to semiconductor theory, the crystal scattering is dominated by ionized impurities. Therefore, it is necessary to fully consider the influence of the relative electron number and electron mobility into the conduction band on the conductivity of SnO_2 to obtain a correct conclusion.

3.2.2. Band and Electronic Effective Mass. The band structure of SnO_2 and different ratios of Ce-doped SnO_2 shown in Figure 3(a) is the band of SnO_2, and Figures 3(b)–3(d) are the band of SnO_2 with the Ce doping ratios of 16.7%, 12.5%, and 8.34%, respectively.

From Figure 3, the bandgap decreases after doping. The band of SnO_2 after doping is introduced in the region of −35 eV~−30 eV new energy level, but this energy level is in the deep-rail region and has little effect on the conductivity. Therefore, we do not consider it. At the same time, new energy levels appear in the doping system near −15 eV and the distribution of electrons increases, providing more electronic states, and the valence band to the conduction band energy level jump probability is greatly increased. Band fluctuations become gentle, indicating that the doping of the electronic locality enhancement. Hence, when SnO_2 is doped with Ce, it makes metal properties to enhance to increase the conductivity of the material.

The electron mobility is inversely proportional to the effective electron mass, and the data derived from two derivation of the band by software are shown in Table 4.

The formula for the effective electron mass is as follows:

$$m_e^* = \frac{h^2}{4\pi^2 d^2 E/dk^2}, \tag{2}$$

where h is the Planck constant, k is the wave vector, and E is the electron energy at the wave vector.

3.2.3. Conductivity Analysis. The following equation is the relationship between the electron mobility μ_i, the doping concentration N_i, and the electron effective mass m_e^*:

$$\mu_i \propto \frac{q}{m_e^* \cdot N_i}. \tag{3}$$

The following equation is derived from the formulas (1)–(3), and the conductivity is proportional to the relative electron concentration and inversely proportional to the doping concentration and the electron effective mass [17]:

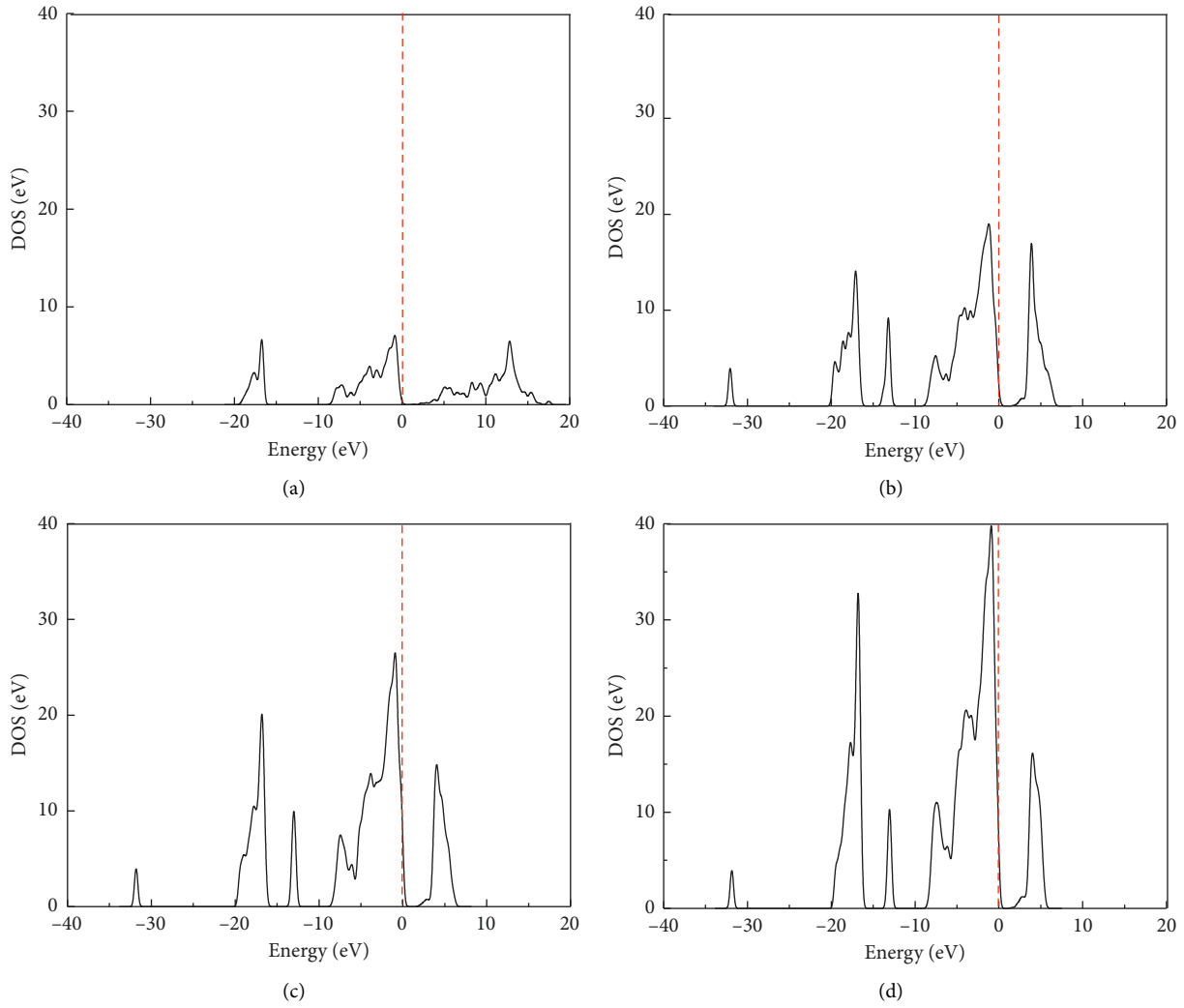

Figure 2: Density of states. (a) SnO_2. (b) 16.7% of Ce-doped SnO_2. (c) 12.5% of Ce-doped SnO_2. (d) 8.34% of Ce-doped SnO_2.

Table 3: Electron concentration.

Ratio	Relative electron number	Relative electron concentration (10^{21} cm^{-3})
16.7%	0.8	9.73
12.5%	1.2	14.7
8.34%	1.6	19.3

$$\delta_i \propto \frac{n_i}{m_e^*.N_i},$$
$$\frac{\delta_i}{\delta_j} = \frac{n_i \cdot m_{ej}^*.N_j}{n_j \cdot m_{ei}^*.N_i}. \quad (4)$$

The doping ratio of 12.5% is used as a reference to get the relative conductivity, as shown in Table 5.

It can be seen from Table 5 that the conductivity of SnO_2 with the Ce doping ratio of 12.5% is the highest.

3.3. Elastic Constant

3.3.1. The Formula for the Elastic Constant. For polycrystalline systems, Hill proved that VRH (Voigt–Reuss–Hill) is closer to the experimental results [18]. The formula for bulk modulus (B) and shear modulus (G) is as follows:

$$B = \frac{(B_V + B_R)}{2},$$
$$G = \frac{(G_V + G_R)}{2}, \quad (5)$$

where B_V and G_V are the elastic modulus and shear modulus of the Voigt model, respectively, and B_R and G_R are the elastic modulus and shear modulus of the Reuss model, respectively. The formula between bulk modulus, shear modulus, and elastic constant C_{ij} ($i, j = 1\sim6$) under the Voigt and Reuss model is as follows [19, 20]:

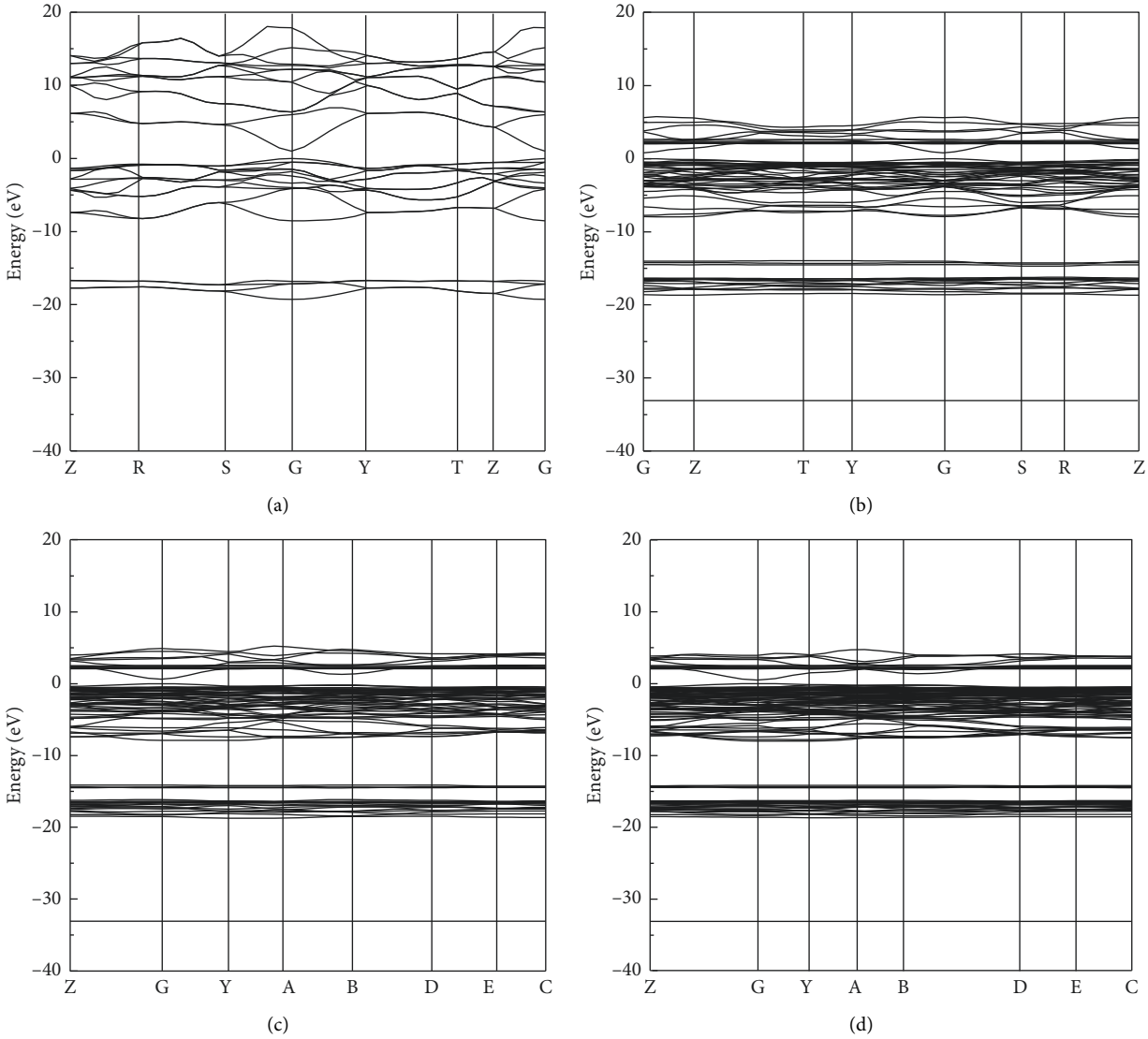

Figure 3: Band structure. (a) SnO_2. (b) 16.7% of Ce-doped SnO_2. (c) 12.5% of Ce-doped SnO_2. (d) 8.34% of Ce-doped SnO_2.

Table 4: Effective electron mass.

Ratio	Two derivation	Effective electron mass (10^{-32} kg)
16.7%	377.9	2.95
12.5%	310.5	3.60
8.34%	148.0	7.44

Table 5: Relative conductivity.

Ratio	Relative Conductivity
16.7%	0.60
12.5%	1
8.34%	0.95

$$B_V = \frac{1}{9}(2C_{11} + C_{33}) + \frac{2}{9}(2C_{13} + C_{12}),$$

$$G_V = \frac{1}{15}(2C_{11} + C_{33} - C_{12} - 2C_{13}) + \frac{1}{5}(2C_{44} + C_{66}),$$

$$B_R = \frac{(C_{11} + C_{12})C_{33} - 2C_{13}^2}{C_{11} + C_{12} + 2C_{33} - 4C_{13}},$$

$$G_R = 15\left(\frac{18B_V}{(C_{11} + C_{12})C_{33} - 2C_{C_{13}}^2} + \frac{6}{C_{13} - C_{12}} + \frac{6}{C_{44}} + \frac{3}{C_{66}}\right)^{-1}. \quad (6)$$

Poisson's ratio (σ) is related to the bulk modulus and the shear modulus as calculated by Hill as follows:

$$\sigma = \frac{3B - 2G}{2(3B + G)}. \quad (7)$$

When studying the mechanical properties of materials, we usually consider the effects of microcracks and lattice distortion on the mechanical properties of materials, and the universal elastic anisotropy index A^{U} is usually the determinant of microcracks and lattice distortion [21]:

$$A^{U} = 5\frac{G_V + B_V}{G_R + B_R} - 6. \quad (8)$$

The Vickers hardness in GPa is evaluated based on the empirical formula of Tian (2012). When the hardness is greater than 5 GPa, the correlation between the empirical formula and the experimentally measured hardness value is quite good. The formula is as follows [22]:

$$H_V + 0.92K^{1.137}G^{0.708}. \quad (9)$$

where $k = G/B$.

3.3.2. Calculation and Analysis of Elastic Constants. In order to study the dynamic stability of the doped system, the corresponding relationship between the elastic constants (C_{ij} (GPa)) of SnO_2 and different ratios of Ce-doped SnO_2 is given in Table 6.

For tetragonal systems, if the dynamics are stable, the elastic constants satisfy the following requirements [23]: $C_{11} > 0$ $C_{33} > 0$ $C_{44} > 0$ $C_{66} > 0$, $C_{11} - C_{12} > 0$ $C_{11} + C_{33} - 2C_{13} > 0$ $2C_{11} + C_{33} + 2C_{12} + 4C_{13} > 0$.

The elastic constants of SnO_2 and different ratios of Ce-doped SnO_2 in Table 6 are calculated, and all satisfy the stability criterion. Therefore, SnO_2 and different ratios of Ce-doped SnO_2 are stable in dynamics.

In order to further predict theoretically the mechanical properties such as hardness (H_V) and crack, the bulk modulus (B), shear modulus (G), hardness (H_V), and universal elastic anisotropy index (A^{U}) values are shown in Table 7.

According to the Pugh criterion, it is generally considered that solid materials with $G/B > 0.57$ are brittle; if they are less than 0.57, it exhibits toughness [24]. From Table 7, the order of G/B values is $SnO_2 > Sn_{0.9166}Ce_{0.0834}O_2 > Sn_{0.875}Ce_{0.125}O_2 > Sn_{0.833}Ce_{0.167}O_2$, which indicates that doping can change the brittleness of the material, and the more the rare earth element Ce, the more obvious the improvement.

Covalent bond orientation directly affects the ability of the material to resist shear strain. Poisson's ratio can reflect the covalent bond orientation problem of internal structure of the material, the lower the value of the former, the stronger the ability of material to resist shear strain. Table 7 shows that Poisson's ratio becomes smaller after doping, indicating that their ability to resist shear strain is enhanced. SnO_2 with the Ce doping ratio of 12.5% has the smaller Poisson's ratio and the best ability to resist shear strain.

Table 6: The relationship between doping ratio and elastic constants

Ratio	C_{11}	C_{22}	C_{33}	C_{44}	C_{55}	C_{66}	C_{12}	C_{13}
0	108.0	108.0	286.1	88.2	88.2	146.8	26.8	41.8
16.7%	243.0	223.2	65.1	68.5	79.5	42.3	−28.3	92.2
12.5%	142.5	277.3	145.5	75.1	134.7	76.0	73.2	58.6
8.34%	147.1	290.6	146.1	79.1	135.9	80.5	74.1	58.1

Table 7: Bulk modulus (GPa), shear modulus (GPa), Poisson's ratio, and universal elastic anisotropy index.

Ratio	B	G	σ	A^{U}	G/B	H_V
0	72.6	82.2	0.26	1.39	1.13	24.0
16.7%	105.2	73.3	0.22	0.93	0.70	13.2
12.5%	103.0	75.5	0.21	0.93	0.73	14.1
8.34%	104.4	78.7	0.20	0.91	0.75	15.5

The index of pervasive elastic anisotropy, A^{U}, is often the decisive factor in the production of cracks. As can be seen from Table 7, the A^{U} values of SnO_2 after doping are smaller and closer than those of SnO_2, indicating that doping has an important effect on improving microcracks.

4. Experimental Preparation of Ag/SnO_2 and Ce-Doped Ag/SnO_2 Contact Materials

4.1. Preparation of Doped SnO_2 Powder by Sol-Gel Method and Ag/SnO_2-Ce Contact Material by Powder Metallurgy. The traditional powder metallurgy method only mixes the doping element powder, SnO_2 powder, and silver powder, which makes it difficult for the doping element to enter the SnO_2 crystal. In order to be consistent with the theoretical calculation model of this paper, the sol-gelation method was used to first prepare different proportions of Ce-doped SnO_2 powder. Then, Ag/SnO_2 and Ce-doped Ag/SnO_2 contact materials were prepared by the powder metallurgy method. The proportion of silver base in each sample was 88%.

4.2. Test of Contact Resistance and Arcing Energy. The electrical contact properties of test materials were tested by using the JF04C electrical contact material tester. 25000 on-off tests were conducted using each pair of contacts. The contact resistance and arcing energy measurement were done every 100 cycles under load 24 V, 13 A, and contact pressure was 86 cN for the on-off period of 0.4 seconds. Finally, the conductivity of the test material is evaluated by the contact resistance and the arcing energy. The arc energy and contact resistance of Ag/SnO_2 doped with different proportions of rare earth elements Ce are shown in Table 8.

Because the rare earth elements easily lose the outermost electrons to form a stable structure with a high melting point, they are not easily decomposed under the action of the arc but accumulate on the surface of the contact, thereby reducing the ablation of the contacts by the arc and reducing the arcing energy.

From Table 8, when the doping ratio is 12.5%, the arcing energy has the smallest variation range, average arcing

Table 8: Arc energy and contact resistance.

Ratio	Arc energy variation range (mJ)	Average arc energy (mJ)	Contact resistance variation range (mΩ)	Average contact resistance (mΩ)
16.7%	173.28~193.91	184.48	0.82~3.87	1.82
12.5%	173.90~189.33	179.31	0.56~2.58	1.24
8.3%	176.49~194.66	184.97	0.60~3.15	1.26
0	159.04~235.28	192.92	0.35~8.93	1.83

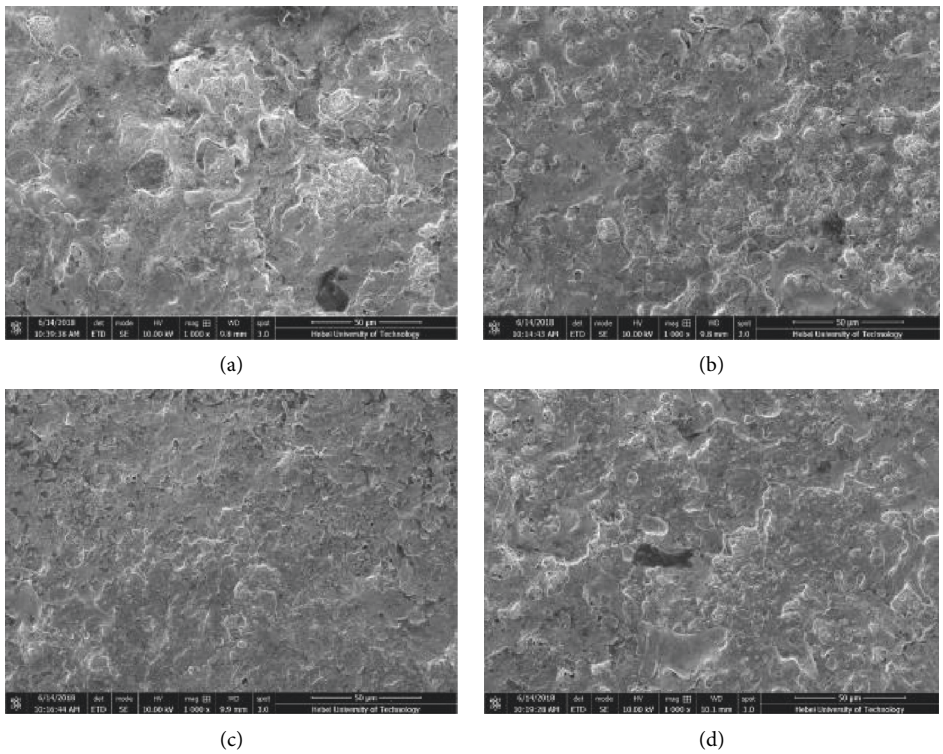

(a) (b) (c) (d)

Figure 4: SEM (a) SnO_2. (b) 16.7% of Ce-doped SnO_2. (c) 12.5% of Ce-doped SnO_2. (d) 8.34% of Ce-doped SnO_2.

energy, and the actual measured conductivity are also the smallest, indicating that Ce-doped SnO_2 has the smallest fluctuation and the most stable.

It is proved that when the rare earth element Ce doping ratio is 12.5%, the electrical properties of the Ag/SnO_2 contact material are the best under the applied test conditions here.

4.3. Microstructure Analysis of Contact Material Surface. Scanning electron microscopy (SEM) was used to observe the arc ablation morphology of the four types of Ag/SnO_2 contact materials, and the arc erosion resistance of the four types of contact materials was analyzed.

After 25,000 electrical contact performance tests of the contact material, the photomicrographs of the contact surface magnified 1000 times are shown in Figure 4, among them Figure 4(a) shows Ag/SnO_2 and Figures 4(b)–4(d) show the Ag/SnO_2 with the Ce doping ratios of 16.7%, 12.5%, and 8.34%, respectively.

The wettability between Ag and SnO_2 particles is poor, which causes the SnO_2 particles to be suspended in the liquid Ag molten pool when the Ag/SnO_2 contact material is in the arc. The surface is easy to form Ag-rich region and SnO_2-rich region. The formation of the Ag-rich region is likely to exacerbate the splash erosion of the contact Ag droplets, and the SnO_2-rich region tends to increase the contact resistance of the contacts. Doping can effectively improve the wettability between Ag liquid and SnO_2 particles so that SnO_2 particles are suspended in the molten system of silver, increasing the viscosity of Ag molten pool, reducing the probability of formation of the SnO_2 polymerization zone, and thus improving the resistance to arc erosion of the Ag/SnO_2 contact material.

Comparing the surface topography of the ablation edge regions of three different proportions of doping, when the doping is 12.5%, the contact surface is flat and without pits, which was because the contact surface shows signs of fluid metal activity after slight melting, and the gap and other phenomena were improved because of the movement of the

flow metal. At this time, the surface is relatively flat and smooth, and the electrical properties are the best. The other two ratios are doped, the surface of the contact has holes, the surface of the molten layer exhibits a flowing state of liquid metal and a mountain pack forms after solidification, and some of the black nonconductive oxides are precipitated.

4.4. Hardness Measurement. The hardness of the sample was measured using the HXD-1000TM digital microhardness tester [17]. The test strength was selected, and the diamond was pressed into the test sample for 5 s. The two diagonal lengths of the diamond indentation on the surface of the sample were observed by a microscope. The hardness value was read, the sample position was changed, and the above process was repeated. Three measurements were made for each sample, and the average value of the hardness was calculated. The hardness values of Ag/SnO_2 and Ag/SnO_2 doped with different proportions of Ce are given in Table 9.

It can be seen from the above table that the more the doping, the lower the hardness. By comparing the theoretical and actual hardness values in Tables 7 and 9, it is found that the simulations and experiments are well matched. From the perspective of the application environment of the contact, high hardness plays an important role in improving the service life of the contact; from the perspective of the forming of the contact, high hardness affects the plasticity and reduces the yield. Therefore, the hardness value must be considered comprehensively.

5. Conclusions

Based on the first principle of density functional theory, the calculated and analyzed results of $Sn_{1-x}Ce_xO_2$ ($x = 0$, 0.083, 0.125, 0.167) show the following:

(1) When the doping proportion of Ce is 0.125, the electron mobility is the highest, and the conductivity and the ability to resist shear strain are the best

(2) When the doping is 0.834, the universal elastic anisotropy index is the smallest

Compared with all performances, 0.125 is the best doping ratio.

Finally, Ag/SnO_2 contacts with different doping ratios were prepared, and arcing energy, contact resistance, and hardness were measured. The final simulation and experimental results can be well matched.

Some people study on Ce-doped Ag/SnO_2 contact material to improve the performance is still in the experimental stage, and the control of the doping amount is also based on the original experience. The innovation of this paper is to obtain the most comprehensive performance by simulating different proportions of Ce doping. A good doping ratio is then verified by experimentation. In the experiment, we not only tested the contact resistance and arc energy but also performed a scanning electron microscope experiment to observe the arc ablation morphology of the contact material. The final theoretical model is well matched to the experiment, providing a method of saving manpower, material resources, and financial resources to improve the electrical properties of Ag/SnO_2 contact materials.

Table 9: Sample hardness measured.

Ratio	16.7%	12.5%	8.3%	0
Hardness (HV)	93.6	100.1	110.9	117.1

Data Availability

The data used to support the findings of this study are included within the article.

Conflicts of Interest

The authors have no conflicts of interest.

Acknowledgments

This study was funded by the National Natural Science Foundation (51777057).

References

[1] H. Li and Y. Hou, "Electro-erosion characteristics of Ag/SnO_2 contact material under DC lamp load," *Electrical Engineering Materials*, vol. 2, pp. 12–15, 2005.

[2] M. Zhang, "Development status of Ag/SnO_2 contact material and its application in relays," *Electrical Engineering Materials*, vol. 4, pp. 20–26, 2004.

[3] Z. Liu, *The Study on Nano-Doped Ag/SnO2 Contact material*, Tianjin University, Tianjin, China, 2007.

[4] S. Tingting, Z. Fuchun, and Z. Weihu, "Density functional theory study on the electronic structure and optical properties of SnO_2," *Rare Metal Materials and Engineering*, vol. 44, no. 10, pp. 2409–2414, 2015.

[5] Y. Zhu, *Study on the Ag/SnO_2 Contact Materials with the Addition of Rare Earth Oxides*, Hebei University of Technology, Tianjin, China, 2007.

[6] Y. Zhu, J. Wang, and L. An, "Preparation and electrical properties of new $Ag/SnO_2/CeO_2$ electrical contact materials," *Rare Metal Materials and Engineering*, vol. 34908, pp. 2011–2014, 2015.

[7] L. Shan, B. Dechun, Y. Lin et al., "The structure and optical properties of Ce-doped SnO_2 materials," *Vacuum*, vol. 1, pp. 25–28, 2014.

[8] Q. Wang, *Research on Tin Dioxide Electrode and its Strengthening and Toughening*, Donghua University, Shanghai, China, 2005.

[9] Q. Wang, *Preparation and Properties of Rare Earth Doped Tin Dioxide Ceramic Electrodes*, Donghua University, Shanghai, China, 2012.

[10] D. Guo and C. Hu, "First-principles study on the electronic structure and optical properties for SnO_2 with oxygen vacancy," *Applied Surface Science*, vol. 258, no. 18, pp. 6987–6992, 2012.

[11] S. F. Matar, D. Jung, and M. A. Subramanian, "The predominance of the rutile phase of SnO_2: first principles study," *Solid State Communications*, vol. 152, no. 5, pp. 349–353, 2012.

[12] M. D. Segall, P. J. D. Lindan, M. J. Probert et al., "First-principles simulation: ideas, illustrations and the CASTEP

code," *Journal of Physics: Condensed Matter*, vol. 14, no. 11, pp. 2717–2744, 2002.

[13] K. G. Godinho, A. Walsh, and G. W. Watson, "Energetic and electronic structure analysis of intrinsic defects in SnO_2," *Journal of Physical Chemistry C*, vol. 113, no. 1, pp. 439–448, 2008.

[14] D. M. Ceperley and B. J. Alder, "Ground state of the electron gas by a stochastic method," *Physical Review Letters*, vol. 45, no. 7, pp. 566–569, 1980.

[15] J. A. Berger, L. Reining, and F. Sottile, "Efficient GW calculations for SnO_2, ZnO and rubrene: the effective-energy technique," *Physical Review B Condensed Matter*, vol. 85, no. 8, article 085126, 2012.

[16] E. Liu, B. Zhu, and J. Luo, *Semiconductor Physics*, Electronic Industry Press, Beijing, China, 6th edition, 2003.

[17] W. Jingqin, Z. Ying, and K. Huiling, "Study on properties of $AgSnO_2$ contact materials doped with rare earth Y," *Materials Research Express*, vol. 5, no. 8, article 085902, 2018.

[18] R. Hill, "The elastic behaviour of a crystalline aggregate," *Proceedings of the Physical Society*, vol. 65, no. 5, pp. 349–354, 2002.

[19] W. Voigt, *Lehrbuch Der Kristallphysik: Teubner*, Macmillan, Leipzig, Germany, 1928.

[20] A. Reuss, "Calculation of the flow limits of mixed crystals on the basis of the plasticity of monocrystals," *ZAMM—Zeitschrift für Angewandte Mathematik und Mechanik*, vol. 9, pp. 49–58, 1929.

[21] S. I. Ranganathan and M. Ostoja-Starzewski, "Universal elastic anisotropy index," *Physical Review Letters*, vol. 101, article 055504, 2008.

[22] Y. Tian, B. Xu, and Z. Zhao, "Microscopic theory of hardness and design of novel superhard crystals," *International Journal of Refractory Metals and Hard Materials*, vol. 33, pp. 93–106, 2012.

[23] F. Zhang, Z. Zhang, W. Zhang et al., "First-principles calculation of the electronic structure and optical properties of In_2O_3," *Journal of Chemistry*, vol. 66, no. 16, pp. 1863–1868, 2008.

[24] Z. Wu, E. Zhao, H. Xiang et al., "Crystal structures and elastic properties of superhard IrN2 and IrN3 from first principles," *Physical Review B*, vol. 76, no. 5, article 054115, 2007.